

## Homogenised model linking microscopic and macroscopic dynamics of a biofilm: Application to growth in a plug flow reactor

C. Deygout<sup>a,b,1</sup>, A. Lesne<sup>c,d</sup>, F. Campillo<sup>a,b</sup>, A. Rapaport<sup>a,b,\*</sup>

<sup>a</sup> EPI INRA-INRIA MODEMIC (*Modelling and Optimisation of the Dynamics of Ecosystems with MICro-organisms*), 2 Place Pierre Viala, 34060 Montpellier Cedex 01, France  
<sup>b</sup> UMR INRA-SupAgro 0729 MISTEA (*Mathematics, Informatics and STatistics for Environmental and Agronomic Sciences*), 2 Place Pierre Viala, 34060 Montpellier Cedex 01, France  
<sup>c</sup> IHÉS (*Institut des Hautes Études Scientifiques*), 35 Route de Chartres, 91440 Bures-sur-Yvette, France  
<sup>d</sup> CNRS UMR 7600 LPTMC (*Laboratoire de Physique Théorique de la Matière Condensée*), UPMC, 4 Place Jussieu, 75252 Paris Cedex 05, France

### ARTICLE INFO

#### Article history:

Received 23 May 2012

Received in revised form 30 October 2012

Accepted 31 October 2012

#### Keywords:

Biofilm  
 Partial differential equations  
 Individual-based model  
 Plug flow reactor  
 Attachment-detachment  
 Advection-diffusion

### ABSTRACT

We propose a new “hybrid” model for the simulation of biofilm growth in a plug flow bioreactor, that combines information from three scales: a microscopic one for the individual bacteria, a mesoscopic or “coarse-grained” one that homogenises at an intermediate scale the quantities relevant to the attachment/detachment process, and a macroscopic one in terms of substrate concentration. In contrast to existing partial differential equations models, this approach is based on a description of biological mechanisms at the individual scale, thus bringing in a biological justification of the attachment/detachment process responsible of the macroscopic behaviour. We found that compared to purely individual based or purely macroscopic models,

- the approximate coarse-grained scale simplifies the change of scales from micro to macro, and speeds up the computation,
- additional information about the stochasticity of the solution, especially at small populations, is revealed compared with the numerical simulations of partial differential equations models.

Furthermore, the coarse-grained model can be much more easily adapted to various attachment/detachment hypotheses, that are at the core of the biofilm development.

© 2012 Elsevier B.V. All rights reserved.

### 1. Introduction

Biofilms are made of complex communities of micro-organisms attached to a surface. They are ubiquitous structures in nature and in industry, where they can have positive roles such as water treatment or negative roles such as material contamination in industrial processes. In the past years, several modelling approaches were used to represent and study biofilms (see Wang and Zhang, 2010 for a general review). One approach is a mathematical description, continuous in time and space, where biofilm development is summed up by a few ordinary or partial differential equations (ODE or PDE, see Wanner et al., 2006; Klapper and Dockery, 2010

for reviews). Using this approach, one is interested in following the whole biofilm at a macroscopic scale in terms of its average concentration over a large surface, with the possibility of some mathematical analyses. Analysis can become very difficult when the models try to take into account hydrodynamics (fluid flow) (e.g. Eberl et al., 2001; Duddu et al., 2009). The other approach is the use of cellular automata (CA) and individual-based models (IBM). In the former, space is discretised into microscopic-sized boxes and the evolution of the contents of each box is described by simple rules, typically involving the contents of neighbouring cells. In the latter, each individual bacterium is studied and can have its own set of rules to follow (with a combination of deterministic and stochastic rules). Using the IBM approach, one is interested in looking at interactions between the individuals at a microscopic scale (see Hellweger and Bucci, 2009; Lapidou et al., 2010 for reviews). Empirical knowledge of the system and its biology can directly be used as the roots of the elementary mechanisms of IBM models. Nevertheless, simulation complexity and runtime can increase very quickly, for example with the number of parameters or that of computer operations. It also means that these models are better suited to study relatively small populations.

\* Corresponding author at: UMR INRA-SupAgro 0729 MISTEA (*Mathematics, Informatics and STatistics for Environmental and Agronomic Sciences*), 2 Place Pierre Viala, 34060 Montpellier Cedex 01, France. Tel.: +33 499612652; fax: +33 467521427.

E-mail address: [alain.rapaport@montpellier.inra.fr](mailto:alain.rapaport@montpellier.inra.fr) (A. Rapaport).

<sup>1</sup> Present address: IRSTEA, UR HBAN (*Hydrosystems et Bioprocédés*), 1 rue Pierre-Gilles de Gennes, CS 10030, 92761 Antony Cedex, France.

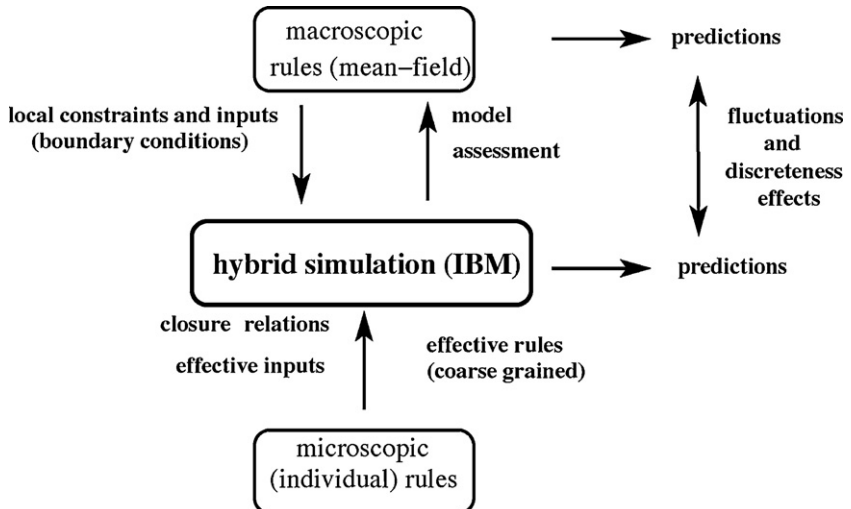


Fig. 1. Double modelling diagram.

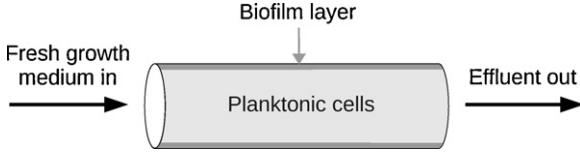


Fig. 2. Flow reactor with biofilm.

In this work, we propose a multiscale model (see Fig. 1) of a 1-dimensional plug-flow reactor, i.e. a long thin tube fed by a laminar flow (Fig. 2), that combines three scales:

- a microscopic description of the growth at the level of individual bacteria, following the well-known Monod law,
- a macroscopic representation of diffusion and advection of the substrate as a continuous concentration (with a discretised gradient and Laplace operator for its numerical simulation, as it is commonly made (Picioreanu et al., 1998)),
- a mesoscopic scale represented by a coarse-grained individual model, in terms of discrete ‘‘boxes’’, that describes the common environment of individual bacteria in each box.

The originality of our approach relies on the introduction of the coarse-grain level which allows to relate the attachment/detachment process of planktonic bacteria with the local density of attached biomass, according to a logistic law. Notice that the size of the boxes has to be large enough for the law of large numbers to hold, but small enough for the homogeneity assumption regarding substrate concentration to hold as well (Fig. 3).

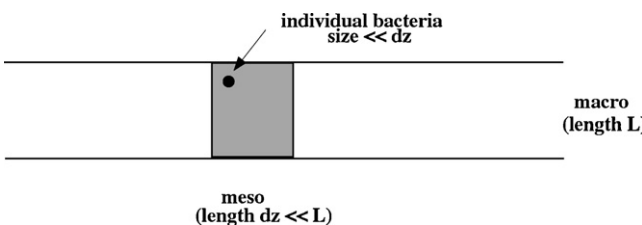


Fig. 3. Definition of the different scales.

## 2. Models

### 2.1. Common hypotheses

Regarding the physical system, we study a plug flow reactor, i.e. a long and thin tube flow reactor as illustrated on Fig. 2. A tube with diameter  $D$  extends along the  $z$ -axis, from  $z=0$  to  $z=L$ . It is fed at  $z=0$  with growth medium by a laminar flow of fluid in the direction of increasing  $z$  and at velocity  $v$  which is constant. The external feed contains all nutrients in non-limiting amounts except one, which is supplied in a constant, growth-limiting concentration  $s_0$ . The flow carries medium, depleted nutrients, bacteria and their by-products out of the reactor at  $z=L$ . Substrate  $s$  is considered to diffuse with coefficient  $d_s$ . We assume negligible variation of nutrient concentration transverse to the axial direction of the tube, because  $D$  is assumed to be small compared to  $L$ .

Regarding the microbial cells, we consider only one bacterial strain. The bacteria can either be suspended in the fluid or attached to the wall. We consider that planktonic bacteria  $P$  have an unbiased random motility superimposed on the advection mechanism. It is similar to regular diffusion and characterised by a diffusion coefficient  $d_P$ . Attached bacteria  $A$  are assumed to be immobile and there is a finite carrying capacity of the wall for attachment. Planktonic bacteria might attach themselves to the wall depending on surface availability, while attached bacteria might detach themselves from the wall. Also, when attached bacteria divide, their daughter-cells might either attach themselves or become planktonic depending on surface availability.

### 2.2. The partial differential equations

Our reference PDE model is a system of equations developed by Ballyk and Smith (1999). This model is an extension of previous ones describing wall growth in chemostat systems (see Ballyk et al., 2008 for a review of these models) based on the work of Freter et al. (1983) on the mammalian gut. The purpose of the extension by Ballyk and Smith (1999) was to account for spatial heterogeneity and material flow. The model accounts for the concentration of substrate  $s(t, z)$ , the concentration of planktonic bacteria  $c_P(t, z)$  and the concentration of attached bacteria  $c_A(t, z)$ . The latter concentration is measured as a weight per surface unit (not per volume unit like the others) as it represents the surface occupied by the attached

bacteria. To convert  $c_A(t, z)$  to the same dimension as  $c_P(t, z)$ , a coefficient called  $\delta$  is used, which is the ratio of the tube surface to the tube volume ( $\delta = (\pi D / (\pi D^2 / 4)) = 4/D$ ).

The equations are the following:

$$\begin{aligned} \frac{\partial s}{\partial t} &= d_s \frac{\partial^2 s}{\partial z^2} - v \frac{\partial s}{\partial z} - c_P f_P(s) \gamma^{-1} - \delta c_A f_A(s) \gamma^{-1} \\ \frac{\partial c_P}{\partial t} &= d_p \frac{\partial^2 c_P}{\partial z^2} - v \frac{\partial c_P}{\partial z} + c_P (f_P(s) - k_p) + \delta c_A f_A(s) (1 - G(C_A)) \dots \\ &\quad - \alpha c_P (1 - C_A) + \delta \beta c_A \\ \frac{\partial c_A}{\partial t} &= c_A (f_A(s) G(C_A) - k_A - \beta) + \alpha c_P (1 - C_A) \delta^{-1} \end{aligned} \quad (1)$$

The substrate uptake rates for planktonic and attached bacteria are given by Monod functions:

$$f_j(s) = \frac{\mu_j s}{K_j + s} \text{ where } j = A \text{ or } P \quad (2)$$

The fraction of daughter-cells of attached bacteria finding sites on the wall,  $G(C_A)$ , depends on the amount of surface available for attachment  $c_{A,\infty}$  with  $C_A = c_A/c_{A,\infty}$  being the fraction of surface already occupied. The main biological requirement on this function is to decrease when  $C_A$  increases and reach zero when  $C_A$  is null. The particular function used since the work of Freter et al. (1983) is the following one:

$$G(C_A) = \frac{1 - C_A}{1 + \epsilon - C_A} \quad (3)$$

where  $\epsilon$  is typically small. We also have the following Danckwerts boundary conditions (Dochain and Vanrolleghem, 2001):

$$\begin{aligned} vs_0 &= -d_s \frac{\partial s}{\partial z}(0, t) + vs(0, t), & \frac{\partial s}{\partial z}(L, t) &= 0 \\ 0 &= -d_p \frac{\partial c_P}{\partial z}(0, t) + vc_P(0, t), & \frac{\partial c_P}{\partial z}(L, t) &= 0 \end{aligned}$$

and the following initial conditions:

$$s(z, 0) = s_{init}(z), \quad c_P(z, 0) = c_{P,init}(z), \quad c_A(z, 0) = c_{A,init}(z), \quad 0 \leq z \leq L$$

normalsize

These equations lead to two possible steady state regimes: complete washout of the bacteria from the reactor and successful colonisation of the reactor by the bacteria. Details about these steady states can be found in Ballyk and Smith (1999). In order to study the system more closely, a numerical approach was used to solve it. We used a similar approach as that used by Ballyk and Smith (1999) with a centered second-order finite difference scheme for diffusion, an upwind first-order finite difference scheme for advection and the semi-implicit Crank–Nicolson method for time.

### 2.3. The microscopic rules

There are two individual-level mechanisms that involve bacterial attachment: attachment of planktonic bacteria and attachment of daughter-cells of attached bacteria. The space available for attachment is assumed to be limited. Any arriving bacterium attaches itself with probability  $\alpha$  if this bacterium is above or next to an available position, else the bacterium becomes or remains planktonic. In order to simplify neighbourhood references, it is possible to homogenise such a mechanism at the mesoscopic scale. Let us consider there are  $X_{max}$  individual positions on the surface in a given neighbourhood, the elementary volume, and already  $X$  individuals occupying some of these positions. We consider two kinds of mechanisms:

- The “homogenised threshold” mechanism (HT). Any arriving bacterium attaches itself with probability  $\alpha$  if there are available positions in the considered space ( $X < X_{max}$ ), else the bacterium

becomes or remains planktonic. This is the most simple description at the mesoscopic level of an elementary volume, without density-dependence effects.

- The “homogenised probability” mechanism (HP). Any arriving bacterium attaches itself with probability  $\alpha(1 - X/X_{max})$ , which means that the bacterium becomes or remains planktonic with probability  $\alpha X/X_{max}$ .

Unless specified otherwise, the IBM is run by default with the HP mechanism for the attachment of planktonic bacteria and the HT mechanism for the attachment of daughter-cells of attached bacteria.

**Remark.** It is interesting to notice that in their equations, Ballyk and Smith (1999) use different mechanisms for the attachment of planktonic bacteria and for the attachment of daughter-cells of attached bacteria. The former is a macroscopic version of the HP mechanism while the latter is of the HT mechanism. These choices are not discussed much in this work (Ballyk and Smith, 1999) nor the references therein. Thus, we have explored these different mesoscopic mechanisms in our coarse-grained IBM and their impact on model results.

## 2.4. The coarse-grained individual-based model

### 2.4.1. Overview

The entities in this model are bacteria. Their microscopic attributes are their position, mass and attachment status. Our main state variables are the number of bacteria in the tube, both attached or detached, as well as the concentration of the substrate. The substrate is not described at a molecular level but its concentration is an attribute of each grid box. The time scale of our simulations is about a few days in duration with a few seconds for the time step. Simulation duration is limited to the time it takes to reach a quasi-steady-state in the system. The time step is constrained by the discretisation scheme used to model the substrate diffusion and advection. The space scale is a few centimetres for the tube length with about 50 µm for the space step.

- The substrate reaction-diffusion process. The substrate in each grid box diffuses horizontally into the two neighbour boxes (the model being pseudo-1D, we assume homogeneity in the directions transverse to the tube axis) and is advected along the flow into the following box (discretised Laplacian). Bacteria in the box eat one after the other in a random order. The speed with which bacteria eat depends on the local substrate concentration and is given by the Monod law (Eq. (2)) as long as substrate is available in the box. The amount eaten by the bacteria increases their mass by that same amount multiplied by the yield factor  $\gamma$ . Substrate concentration in the boxes is updated only at the end of these steps (see Fig. 4). Despite the artificiality of this sequence, discrepancies should be small because the time step remains very small.
- The bacteria division process. Bacteria that have a mass higher than the division threshold  $m_{div}$  divide into two bacteria of total mass that of the mother bacteria (see Fig. 5).
- The bacteria attachment/detachment process. The detached bacteria are advected by the flow and have a random horizontal motility (see Fig. 6). The different attachment processes are described in Section 2.3.

### 2.4.2. Description

The work is based on that of Mabrouk et al. (2010), Mabrouk (2010), itself based on similar assumptions as that of Picioreanu et al. (1998) or Kretf et al. (2001). Main differences regard the presence of a flow and taking the border into account.

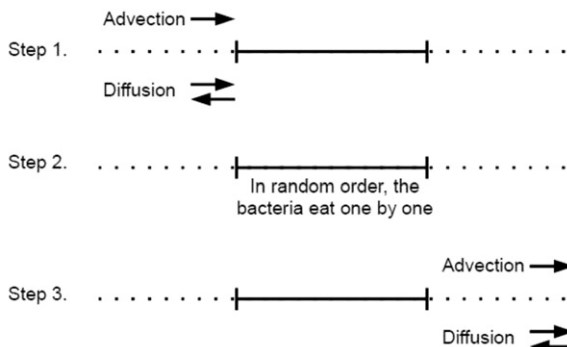


**Fig. 4.** Diagram illustrating the rules of substrate change at each time step, in each box along the tube.

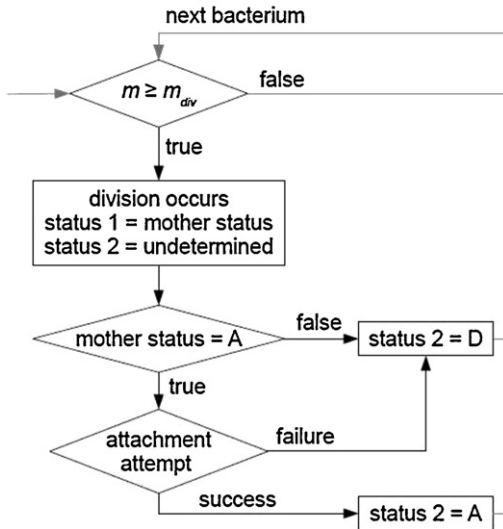


**Fig. 5.** Diagram illustrating the rules of bacterial division at each time step, for each bacterium. Attachment status: A, attached; D, detached.

Given the small time scale of our simulations, the bacteria in this model do not have adaptive traits and hence do not attempt to meet objectives. They have no learning abilities and do not attempt to predict their future environment.

**2.4.2.1. Initialisation and inputs.** Before the simulation starts, a number of bacteria are placed in the boxes (location picked from a random uniform distribution), a certain number of which are attached ( $N_{A,\text{init}}$ ), the others detached ( $N_{P,\text{init}}$ ). Each bacterium has an initial mass of  $m_{\text{init}}$ . Substrate is present throughout the tube at a given concentration  $s_{\text{init}}$ .

The input data, such as bacteria initial position, are chosen randomly. Nevertheless, if one wanted to specifically reproduce a given part of a larger tube, initial conditions of the model could be forced to resemble any point of the PDE system representing the whole tube.

#### 2.4.2.2. Bacterial biology and movement.

**2.4.2.2.1. Growth.** Each bacterium consumes a given amount of substrate which is determined by the Monod growth kinetics and its own mass  $m$ . We assume that bacterial growth is directly equal to this amount consumed, multiplied by the conversion yield factor  $\gamma$ . At time  $t$  and in box  $i$ , the increase in mass  $dm$  is the following:

$$dm = \gamma m \frac{\mu_j s_{t,i}}{K_j + s_{t,i}}$$

where  $j$  is either  $A$  or  $P$  for attached or planktonic bacteria respectively (see Table 1 for more details).

**2.4.2.2.2. Division.** Each bacterium that has a mass higher than the division threshold  $m_{\text{div}}$  divides into two bacteria of total mass that of the mother bacterium. Each of the two daughter-bacteria receives half of the mother mass plus or minus a random amount (taken from a uniform distribution between 0 and 25% of the mother mass). One of the daughter bacteria retains the mother location and attachment status, and the other bacterium has the same location plus or minus a random amount (taken from a uniform distribution between 0 and mother diameter). That second daughter bacterium has the same attachment status as its mother by default. If that status is attached, depending on the mechanism used for attachment (see Section 2.3), then the new bacterium might become detached. A daughter bacterium which location is outside the tube is considered as washed out.

**2.4.2.2.3. Attachment and detachment.** Each of the detached bacteria has a probability involving  $\alpha$  times  $dt$  and  $m_{A,\infty}$  to attach itself on the wall. The exact mechanism can be varied according to the description in Section 2.3. Each of the attached bacteria has a probability  $\beta$  times  $dt$  to detach itself.

**2.4.2.2.4. Movement.** The detached bacteria are advected by the flow and have a random horizontal motility modelled as a

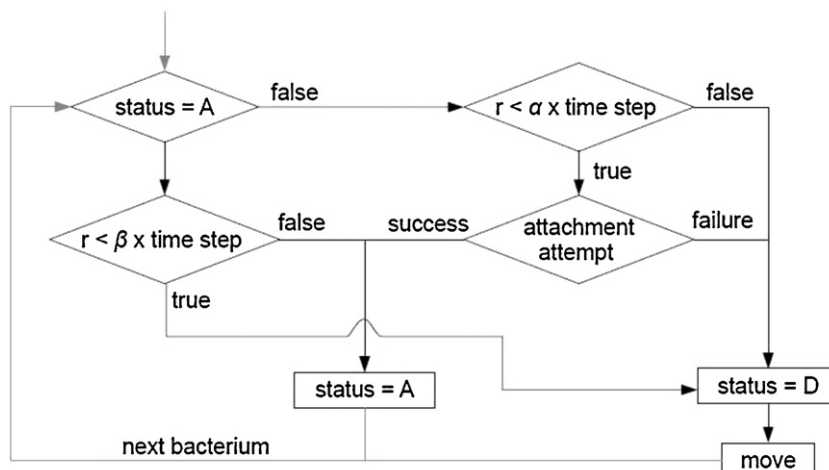


**Fig. 6.** Diagram illustrating the rules of bacterial attachment or movement at each time step, for each bacterium. Attachment status: A, attached; D, detached; r, number drawn each time from a uniform distribution between 0 and 1.  $\alpha$  and  $\beta$  are respectively the attachment and detachment rates.

**Table 1**

Description of the symbols used in both models, with units shown in brackets.

Description	PDE symbol	IBM symbol	Default value
Space	Continuous position $z$ [m]	Box number $i$ , space step $dz$ [m]	200 boxes
Time [s]	Continuous time $t$	Discrete time $t$ , time step $dt$	–
Substrate concentration [ $\text{kg m}^{-3}$ ]	$s(t, z)$	$s_{t,i}$	–
Amount of planktonic bacteria	Concentration $c_P(t, z)$ [ $\text{kg m}^{-3}$ ]	Number $N_{P,t,i}$ or mass $m_{P,t,i}$ [kg]	–
Amount of attached bacteria	Concentration $c_A(t, z)$ [ $\text{kg m}^{-2}$ ]	Number $N_{A,t,i}$ or mass $m_{A,t,i}$ [kg]	–
Initial substrate concentration	$s_{init}$	$s_{init}$	$1 \times 10^{-3} \text{ kg m}^{-3}$
Initial amount of $j$ -type bacteria <sup>a</sup>	Concentration $c_{j,init}$ [ $\text{kg m}^{-2}$ ]	Number $N_{j,init}$	1000 ind.
Length of tube	$L$	$L$	0.01 m
Diameter of tube	$D$	$D$	$1 \times 10^{-3} \text{ m}$
Flow velocity	$v$	$v$	$1 \times 10^{-6} \text{ m s}^{-1}$
Conversion yield	$\gamma$	$\gamma$	1
Ratio of tube circumference to cross-sectional area	$\delta$	–	$4 \times 10^3 \text{ m}^{-1}$
Input substrate concentration	$s_0$	$s_0$	$1 \times 10^{-3} \text{ kg m}^{-3}$
Attachment rate	$\alpha$	$\alpha^b$	$1 \times 10^{-8} \text{ s}^{-1}$
Detachment rate	$\beta$	$\beta^b$	$1 \times 10^{-5} \text{ s}^{-1}$
Diffusion rate of substrate	$d_s$	$d_s^b$	$1 \times 10^{-14} \text{ m}^2 \text{ s}^{-1}$
Diffusion rate of planktonic bacteria	$d_P$	$d_P^b$	$1 \times 10^{-13} \text{ m}^2 \text{ s}^{-1}$
Maximum growth rate of $j$ -type bacteria <sup>a</sup>	$\mu_j$	$\mu_j^b$	$1 \times 10^{-4} \text{ s}^{-1}$
Half-saturation constant for $j$ -type bacteria <sup>b</sup>	$K_j$	$K_j^b$	$1 \times 10^{-3} \text{ kg m}^{-3}$
Maximum amount of attached bacteria	Concentration $c_{A,\infty}$ [ $\text{kg m}^{-2}$ ]	Mass $m_{A,\infty}$ [kg]	$1 \times 10^{-10} \text{ kg}$
Wall fraction occupied by attached bacteria	$C_A = c_A/c_{A,\infty}$	$M_A = m_A/m_{A,\infty}$	–
Dimensionless coefficient of $G(C_A)$	$\epsilon$	–	0.01
Fraction of daughters of attached bacteria finding sites on the wall	$G(C_A) = \frac{1-C_A}{1+\epsilon-C_A}$	–	–
Initial individual mass	–	$m_{init}$	$1 \times 10^{-15} \text{ kg}$
Mass over which an individual divides	–	$m_{div}$	$2 \times 10^{-15} \text{ kg}$

<sup>a</sup>  $j = P$  for planktonic bacteria or  $A$  for attached bacteria; here  $P$  and  $A$  parameters have the same values.<sup>b</sup> Same coefficient in both models but may be used slightly differently to account for discretisation.

Brownian motion process with an apparent diffusion factor  $d_P$ . The distance crossed over one time step thus follows a Gaussian law of variance twice the diffusion-like factor  $d_P$  multiplied by the time step (Mabrouk, 2010).

## 2.5. Numerical experiments

We ran a large number of numerical experiments for both the PDE system and the IBM. Parameter values are those indicated in Table 1 unless mentioned otherwise. In the case of the PDE system, one run gives the deterministic output for a given set of parameters. But in the case of the IBM, twelve runs were made with different random seeds. This is in contrast with classical Monte Carlo techniques that require a greater number of simulations to infer the average behaviour and the deviation from this average behaviour. Our situation is indeed different as we consider jointly a PDE model and an IBM. This latter model tends to various types of PDE or integro-differential equation models depending on how the different discretization steps tend toward 0 and what type of rescaling is adopted. In particular, the PDE considered here is one of the limit models of the IBM. Hence the IBM simulator is not intended here to be used as a Monte Carlo technique to infer an average behaviour from a large number of simulations. It has rather the status of an in silico experimentation tool, and in terms of experimentation, twelve is a large number. This number of simulations is sufficient to determine how the PDE model deviates from the in silico experimentations but more importantly to understand the qualitative nature of this discrepancy. We study the following result variables once the steady state is reached (large  $t$ ):

- the profiles along the tube for all three variables (in terms of mass, for comparison between the two models);
- the biofilm “length”, which is defined as  $\arg\max_i(m_{A,t,i} - m_{A,t,i-1})$ , i.e. the location  $i$  along the tube where the difference between two following positions is maximum;
- the sum over the whole tube of the attached biomass.

## 3. Results

### 3.1. General description of steady state profiles

In both models, we find similar profiles at the steady state for the default values (Fig. 7). These profiles indicate an important development of the biofilm in the leftmost side of the tube where the nutrient flow enters. Parallel to this biofilm development which reaches the carrying capacity, there is an important decrease in substrate concentration. Once a threshold substrate concentration is crossed, there is not enough substrate to allow the growth of a thick biofilm and the amount of attached bacteria reaches a value close to one bacterium along the remainder of the tube. Meanwhile, the amount of detached bacteria increases along the whole tube, these bacteria being released by the thick biofilm of the leftmost part of the tube.

There are nevertheless differences between the two models. First of all, in the right-most part of the tube, there are few attached

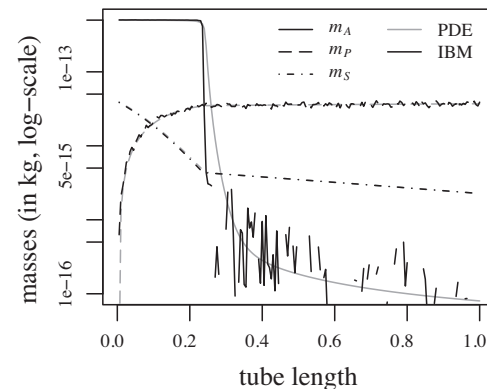


**Fig. 7.** General profile along the tube observed at the steady state for the PDE numerical resolution (gray lines) and the average over 12 IBM runs (black lines) with default values as shown in Table 1. The mass of attached bacteria  $m_A$  is represented by solid lines, the mass of planktonic bacteria  $m_P$  by dash-dot lines and the mass of substrate  $m_S$  by long dashes. The horizontal axis is the length of tube divided by  $L$ .

bacteria and the two models represent this situation differently. The IBM gives a presence-absence information: there is no point in case no attached bacteria are present due to the log-scale of Fig. 7. Meanwhile, the PDE gives a continuous expression which in the right-most part of the graph corresponds to about a tenth of an individual bacterium. Nevertheless, both cases give similar values. Second, the attached bacteria in the thick biofilm are slightly more developed in the IBM than in the PDE, which implies a slightly shorter biofilm length. The difference in biofilm length is exaggerated by the log-scale but it remains quite small (about 1 “box” of difference) and the difference in overall attached biomass is about 2%. Third, the change from thick biofilm to little or no biofilm is quite sharp in both cases but it is even sharper in the IBM. Finally, there is also the effect of fluctuations in the IBM to be considered. This variability does not reflect individual variance because there has already been some homogenisation but it could be thought of as a “quality” assessment of the coarse-grained IBM. Overall, the variance along the profile is relatively low, in particular for the substrate concentration and the planktonic bacteria. Indeed, these two elements are affected by diffusion processes which smooth their distribution along the tube and there is less variability between runs. For the attached biomass, it is quite low over the thick biofilm length but increases afterwards, in particular over the switch from thick biofilm to almost no attached bacteria (data not shown).

### 3.2. Parallel between discretisation to solve PDE and discretised events in IBM

In both cases, whether the model was conceived in a continuous or a discrete manner, the resulting simulations relied on a discretised code. Thus, in both cases, we can compare the impact of the number of spatial boxes making up the whole tube. By keeping the tube length constant and increasing the number of boxes, the size and volume of each box is reduced. Using a large number of boxes increases the similarity of the results with those that might be obtained with a continuous representation. But it also increases simulation run time and it reduces the number of individuals or biomass present in each box which may lead to observing quantities smaller than one individual in the case of the PDE system. In this work, we find that the numerical experiments are relatively resilient to the number of boxes and thus to box size as well (Fig. 8). By using a small number of boxes, there is a slight tendency to overestimate the biofilm length in both models, but the difference remains well under 1%. Also, this is more apparent for the PDE system than for the IBM.

### 3.3. Sensitivity analysis

Sensitivity analysis generally refers to any investigation intending to check the robustness of the model predictions with respect to a change in the model features. Following the methodological review by Cariboni et al. (2007), we distinguish the sensitivity to model parameters, the uncertainty due to model stochasticity, and the structural stability (or instability) with respect to a qualitative change in the implementation or modelling choices. The uncertainty due to inherent stochasticity has been appreciated by running the simulation with different random seeds (Section 2.5). The influence of the size of the spatial boxes used in the homogenisation has been treated in Section 3.2 (see in particular Fig. 8). The influence of the attachment/detachment rules will be treated in Section 3.4 (see in particular Fig. 12). We have also checked the insensitivity to the division rules. In the present section, we dissect to the sensitivity of the simulation results by varying the main parameters ( $s_0$ ,  $v$ ,  $m_{A,\infty}$ ,  $\mu_j$ ,  $K_j$ ,  $\alpha$ ,  $\beta$ ) independently, one at a time. This approach is tractable thanks to the minimal nature of our

model, making possible to control and understand the impact of each term.

Overall, the same effects are observed on PDE and IBM simulations. Differences in the main results (length of biofilm, mass of attached bacteria) between the two models remained well under 5%. The parameters tested here are those which have a major impact on the results.

An increase in the concentration substrate  $s_0$  leads to an increase in the length of biofilm formed (first line of Fig. 9). An increase in the flow velocity  $v$  leads to a similar effect. Indeed, increasing  $v$  leads to an increased amount of substrate available for the bacteria. An increase in the maximum amount of attached bacteria  $m_{A,\infty}$  leads to a decrease in the length of biofilm which is formed (second line of Fig. 9). Indeed, since the biofilm is thicker, the substrate is completely eaten earlier along the tube and prevents further biofilm development.

As regards the parameters of the growth curves, an increase in both  $\mu_j$  or both  $K_j$  leads first to an increase in the length of biofilm formed and after reaching a peak value it leads to a decrease (Fig. 10). Indeed, for low values of  $\mu_j$ , bacteria are washed out while for high values of  $\mu_j$ , the bacteria are very efficient in eating the substrate and only a short length of biofilm can develop before the tube is emptied of substrate. Thus, it is for intermediate values of  $\mu_j$  that a maximum length of biofilm is observed. Similar results are observed for  $K_j$  but with high values of  $K_j$  leading to a wash-out and low values of  $K_j$  leading to a short and efficient biofilm.

An increase in the attachment rate  $\alpha$  has very little effect on the development of the main biofilm in the leftmost part of the tube. Nevertheless, it leads to an increase in the development of the biofilm in the rest of the tube (Fig. 11). Bacteria in this part of the biofilm do not grow because there is very little substrate left but the biofilm is built via attachment of planktonic bacteria flowing by. An increase in the detachment rate  $\beta$  leads to a decrease in the length of biofilm formed (Fig. 11). Indeed, for large values of  $\beta$ , the amount of substrate needed for biofilm development (including compensation for biofilm detachment) is higher than for smaller values of  $\beta$ . For a large enough value of  $\beta$ , there is wash-out.

### 3.4. Impact of microscopic attachment mechanisms

Different attachment mechanisms were considered (Fig. 12). The PDE mechanism of the  $G$  function and the “homogenised threshold” (HT) mechanism lead to similar macroscopic behaviours, with an abrupt limit to attachment possibilities for bacteria and thus an abrupt distinction between a part of the tube with a thick biofilm and the other part with almost no attached bacteria. Whichever mechanism is followed for the attachment of planktonic bacteria, the results are similar because this attachment is mostly important in the part of the tube with little attached bacteria and thus for values where all mechanisms behave similarly. On the other hand, whether the attachment of daughter bacteria follows the HT or the HP mechanism has a much more important impact on the overall profile along the tube. Indeed, the “homogenised probability” (HP) mechanism leads to a much smoother transition between the part of the tube with a thick biofilm and the other part with almost no attached bacteria. It remains to be seen which may be the more realistic approach.

## 4. Discussion

### 4.1. Modelling choices

Multiscale approaches in physics mainly aim at extracting macroscopic dynamics from a more microscopic description (Givon et al., 2004). Mathematical methods are available when the

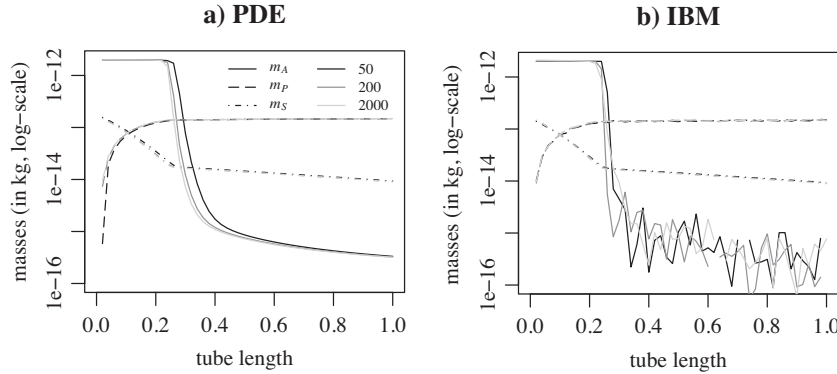


**Fig. 8.** Effect of the number of boxes on the steady state profile for (a) the PDE numerical resolution and (b) the average over 12 IBM runs. The values for the number of boxes are: 50 in black, 200 in dark grey and 2000 in light grey. The mass of attached bacteria  $m_A$  is represented by solid lines, the mass of planktonic bacteria  $m_P$  by long dashes and the mass of substrate  $m_S$  by dash-dot lines. The horizontal axis is the box coordinate along the tube divided by  $L$ .

microscopic dynamics is already described with an analytical ODE or PDE formalism, mainly based either on a decomposition in slow and fast variables (see e.g. the review in Lesne, 2006), or an averaging of microscopic quantities and their dynamics (e.g. derivation of rate equations Acharya and Sawant, 2006), or an homogenisation of the microscopic details (see e.g. the monograph Torquato, 2002). In the case where microscopic dynamics is accessible to simulation only, we suggest to adapt homogenisation methods. However, considering only a macroscopic description is not sufficient because local spatial structures and local behaviours matter.

We thus consider a mesoscopic (or “coarse-grained”) scale that homogenises at an intermediate scale the attachment/detachment process of the biofilm, while keeping track of the discrete nature of

bacterial cells and their individual location, growth and division. In this respect our model can also be termed “hybrid”: it is at the same time discrete (spatial location, growth and division of each bacterial cell, to account accurately to their participation to the biofilm spatial structure), and continuous (same rules in a spatial cell, as if we were considering a population of cells, described by a single set of continuous quantities). Homogenisation is here achieved by endowing each bacterial cell with the average behaviour (average in a spatial cell) as regards the attachment and detachment processes. Our mesoscopic account of these processes involves bacteria densities and effective rates, which makes possible a direct derivation of the corresponding term in a PDE description (provided that statistical averages and macroscopic densities are identified). In

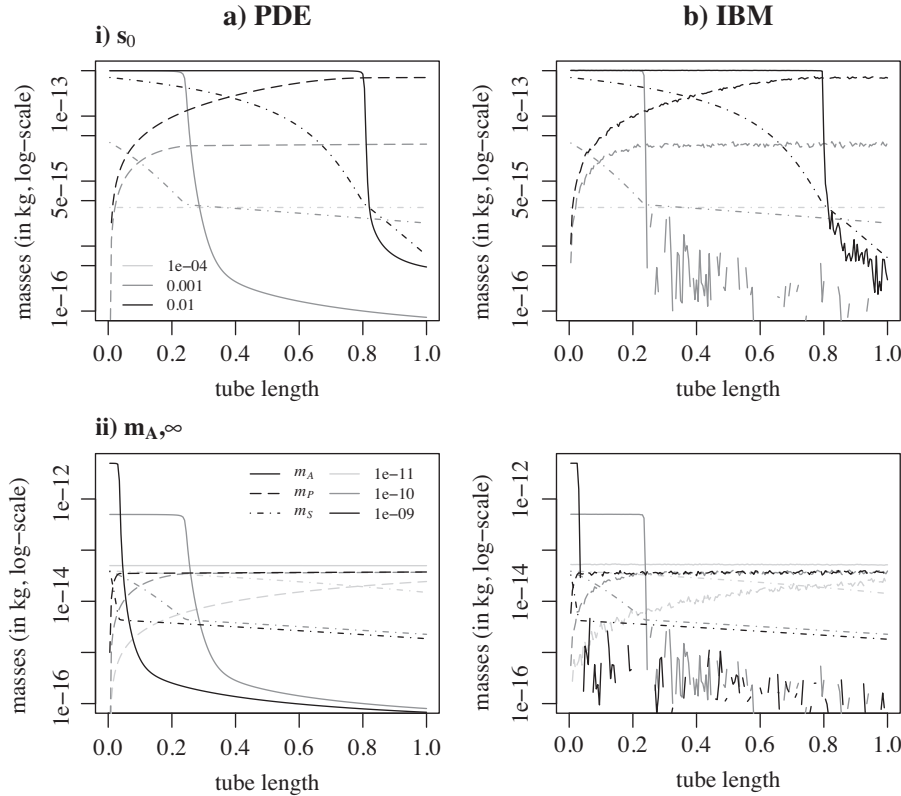


**Fig. 9.** Effect of (i) the input concentration of substrate  $s_0$  and (ii) the maximum amount of attached bacteria  $m_{A,\infty}$  on the steady state profile for (a) the PDE numerical resolution and (b) the average over 12 IBM runs. The values for  $s_0$  are:  $1 \times 10^{-4}$  in light grey,  $1 \times 10^{-3}$  in dark grey and  $1 \times 10^{-2}$  in black (in  $\text{kg m}^{-3}$ ). The values for  $m_{A,\infty}$  are:  $1 \times 10^{-11}$  in light grey,  $1 \times 10^{-10}$  in dark grey and  $1 \times 10^{-9}$  in black (in kg). The mass of attached bacteria  $m_A$  is represented by solid lines, the mass of planktonic bacteria  $m_P$  by long dashes and the mass of substrate  $m_S$  by dash-dot lines. The horizontal axis is the box coordinate along the tube divided by  $L$ .

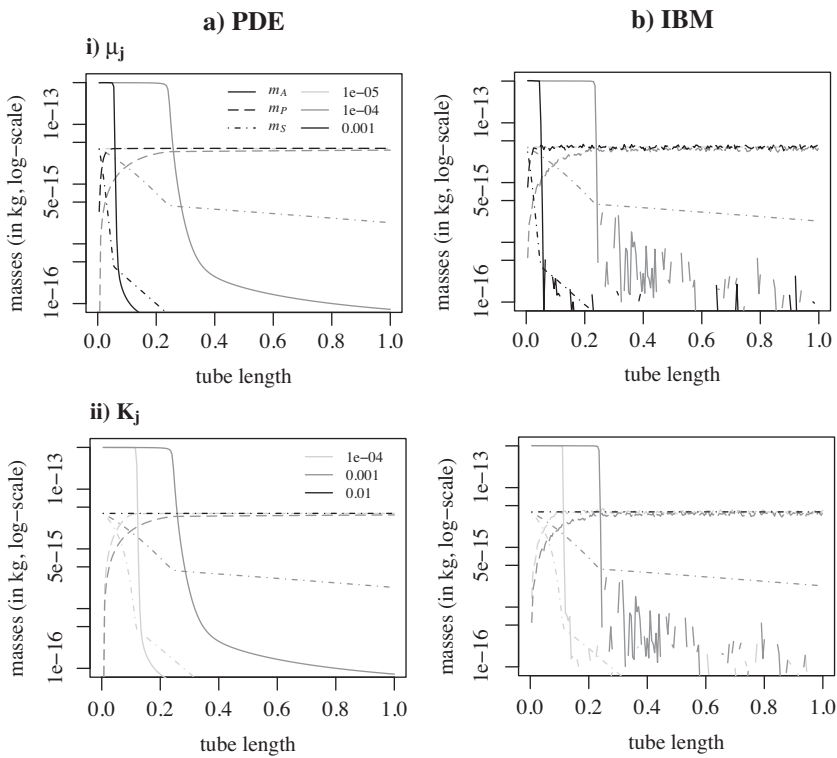


**Fig. 10.** Effect of (i) both  $\mu_j$  or (ii) both  $K_j$  on the steady state profile for (a) the PDE numerical resolution and (b) the average over 12 IBM runs. The values for  $\mu_j$  are:  $1 \times 10^{-5}$  in light grey,  $1 \times 10^{-4}$  in dark grey and  $1 \times 10^{-3}$  in black ( $\text{in s}^{-1}$ ). The values for  $K_j$  are:  $1 \times 10^{-4}$  in light grey,  $1 \times 10^{-3}$  in dark grey and  $1 \times 10^{-2}$  in black ( $\text{in kg m}^{-3}$ ). The mass of attached bacteria  $m_A$  is represented by solid lines, the mass of planktonic bacteria  $m_P$  by long dashes and the mass of substrate  $m_S$  by dash-dot lines. The horizontal axis is the box coordinate along the tube divided by  $L$ .

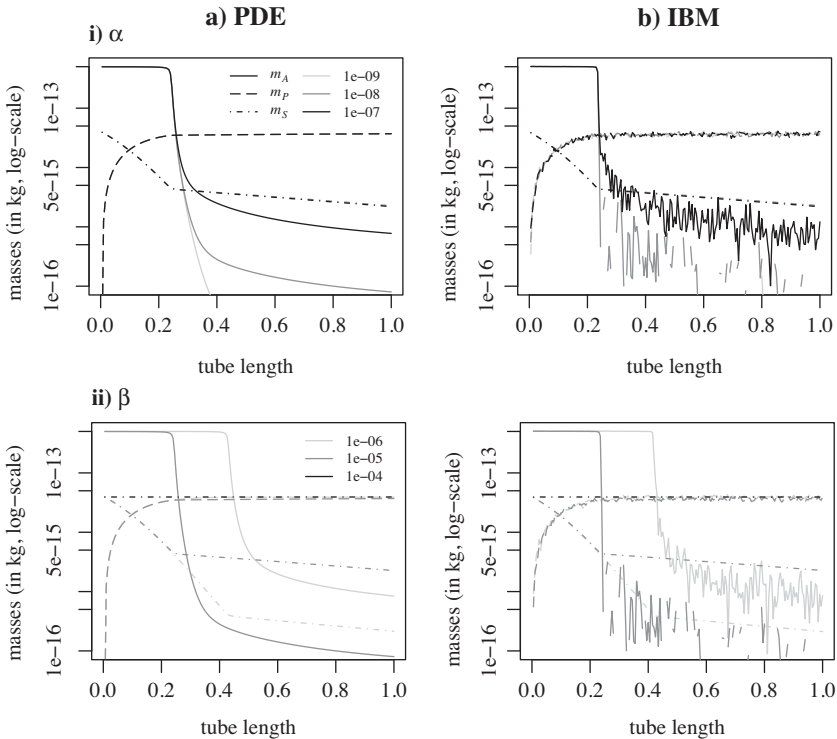


**Fig. 11.** Effect of (i)  $\alpha$  and (ii)  $\beta$  on the steady state profile for (a) the PDE numerical resolution and (b) the average over 12 IBM runs. The values for  $\alpha$  are:  $1 \times 10^{-9}$  in light grey,  $1 \times 10^{-8}$  in dark grey and  $1 \times 10^{-7}$  in black ( $\text{in s}^{-1}$ ). The values for  $\beta$  are:  $1 \times 10^{-6}$  in light grey,  $1 \times 10^{-5}$  in dark grey and  $1 \times 10^{-4}$  in black ( $\text{in s}^{-1}$ ). The mass of attached bacteria  $m_A$  is represented by solid lines, the mass of planktonic bacteria  $m_P$  by long dashes and the mass of substrate  $m_S$  by dash-dot lines. The horizontal axis is the box coordinate along the tube divided by  $L$ .

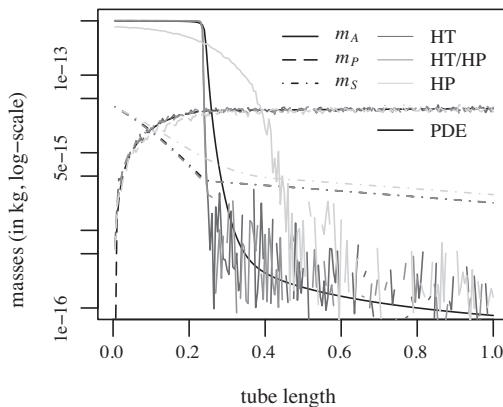


**Fig. 12.** Comparison of different mechanisms for the attachment of bacteria in the IBM (various dashed and dotted lines) with the reference PDE (solid black lines) at the steady state. In the IBM, the PDE mechanism of the  $G$  function and the “homogenised threshold” (HT) mechanism give similar results whether used for the attachment of planktonic or daughter bacteria and their results are thus both represented by the dark grey lines. The medium grey lines represent the use of the “homogenised threshold” (HT) mechanism for the attachment of daughter bacteria and/or of the “homogenised probability” (HP) for the attachment of planktonic bacteria in the IBM. The light grey lines represent the use of the “homogenised probability” (HP) mechanism for both kinds of attachment in the IBM. The mass of attached bacteria  $m_A$  is represented by solid lines, the mass of planktonic bacteria  $m_P$  by long dashes and the mass of substrate  $m_S$  by dash-dot lines. The horizontal axis is the box coordinate along the tube divided by  $L$ .

this way, our simulation model combines information from three scales: spatial distribution and growth of individual bacterial cells, homogenised view of the attachment and detachment processes, and a comparison with PDE solutions at macroscopic scale. The latter moreover provides a way to appreciate the validity of the macroscopic description at small numbers of cells.

#### 4.2. Perspectives

Using an IBM approach to describe this plug-flow system has several advantages. First of all, it allows us to use “biological” rules, i.e. rules that can intuitively be suggested (and tested) by biologists based on their in-depth knowledge of the real system. This makes the system more amenable to interactions with experiments and also to changes in the choice of mechanisms. This IBM may thus lead to improvement over the original model proposed by Freter et al. (1983) and its variations (Ballyk and Smith, 1999) by allowing us to test mechanisms that could not be easily formulated or even solved analytically. One possibility would be to explore the biofilm dynamics when considering different bacterial strains competing inside the tube for space and/or substrate resources. Also, we could consider taking into account the (transversally) inhomogeneous velocity profile through a shear rate, generating a shear force on attached bacteria which would promote their detachment (with an effect on the  $\beta$  parameter) and limit the thickness of biofilm (effect on the  $c_{A,\infty}$  carrying capacity parameter).

Regarding the density issue (thick biofilm in one part of the tube, few attached bacteria in the other part), we could consider an association of the different models, in the spirit of the heterogeneous multiscale method of E and collaborators (Weinan and Engquist, 2003; Weinan et al., 2009). Indeed, currently we have compared the PDE and IBM models but a prospect could be to use them sequentially with the PDE at the start of the tube where the population is larger and a transition to the IBM for the rest of the tube where the population is smaller.

Our homogenised IBM could be extended in two directions to fully model the *ecological* dynamics of the biofilm: first by taking into account complex interactions between individuals, second

by capturing in its dynamic rules the influence of the emergent properties of the biofilm on the individual features and behaviour (e.g. geometrical or mechanical constraints). It provides the framework to investigate the multiscale organisation of the biofilm, encompassing both emergent collective features (bottom-up integration) and top-down influences (modification of the individual or homogenised dynamics of bacterial cells embedded in the biofilm) (Lesne, in press).

#### 4.3. Conclusion

We have proposed a new multiscale model of biofilm growth in a plug flow reactor, with reasonable runtimes for the simulations while remaining close to microscopic processes and knowledge. In particular, our approach focuses on the hypotheses regarding the attachment/detachment process that is at the core of biofilm growth. The comparison with the PDE model has led to similar steady-state concentration profiles at the macroscopic level.

From the biologist or microbial ecologist viewpoint, this modelling approach present several advantages compared to more traditional approaches based on macroscopic population models:

- It describes the biological mechanisms at the individual scale, closer to what is known or observed experimentally by biologists, and uses meaningful biological parameters.
- It allows to justify biologically (or not) some terms that are chosen in the PDE model without direct macroscopic justification, especially the terms related to attachment/detachment process in biofilms.
- It provides additional information on second-order terms or variance around the average profile that have been compared with the PDE model. This brings insight about the variability of biofilm features and dynamics depending on the values of the parameters and the size of the populations.

From a methodological viewpoint, the curse of dimensionality inherent to individual-based models has been reduced by the consideration of a mesoscopic or “coarse-grained” scale. This framework is thus generic and efficient. It is suitable for investigating from the level of microscopic details to that of macroscopic predictions multispecies biofilms in more complicated two or three dimensional geometries. It has the potential to model ecological processes such as complex interactions between individuals or the influence of the emergent properties of the biofilm on the individual features and behaviour.

#### Acknowledgments

This work has been achieved within the DISCO (“multiscale modelling bioDIversity Structure COpling in biofilms”) project of the French Agency of Research SYSCOMM program (ANR AAP215-SYSCOMM-2009), that has funded CD’s postdoctoral fellowship.

#### References

- Acharya, A., Sawant, A., 2006. On a computational approach for the approximate dynamics of averaged variables in nonlinear ode systems: toward the derivation of constitutive laws of the rate type. *Journal of the Mechanics and Physics of Solids* 54 (10), 2183–2213.
- Ballyk, M., Smith, H.L., 1999. A model of microbial growth in a plug flow reactor with wall attachment. *Mathematical Biosciences* 158 (2), 95–126.
- Ballyk, M., Jones, D., Smith, H.L., 2008. The biofilm model of Freter: a review. In: Magal, P., Ruan, S. (Eds.), *Structured Population Models in Biology and Epidemiology*. Springer Edition, Berlin, pp. 265–302.
- Cariboni, J., Gatelli, D., Liska, R., Saltelli, A., 2007. The role of sensitivity analysis in ecological modelling. *Ecological Modelling* 203 (1–2), 167–182.
- Dochain, D., Vanrolleghem, P., 2001. *Dynamical modelling and estimation in wastewater treatment processes*. IWA Publishing, Padstow, UK.

- Duddu, R., Chopp, D.L., Moran, B., 2009. A two-dimensional continuum model of biofilm growth incorporating fluid flow and shear stress based detachment. *Biotechnology and Bioengineering* 103 (1), 92–104.
- Eberl, H.J., Parker, D.F., van Loosdrecht, M.C.M., 2001. A new deterministic spatio-temporal continuum model for biofilm development. *Journal of Theoretical Medicine* 3 (3), 161–175.
- Freter, R., Brickner, H., Fekete, J., Vickerman, M.M., Carey, K.E., 1983. Survival and implantation of *Escherichia coli* in the intestinal tract. *Infection and Immunity* 39 (2), 686–703.
- Givon, D., Kupferman, R., Stuart, A., 2004. Extracting macroscopic dynamics: model problems and algorithms. *Nonlinearity* 17, 55–127.
- Hellweger, F.L., Bucci, V., 2009. A bunch of tiny individuals – individual-based modeling for microbes. *Ecological Modelling* 220 (1), 8–22.
- Klapper, I., Dockery, J., 2010. Mathematical description of microbial biofilms. *SIAM Review* 52 (2), 221–265.
- Kreft, J.-U., Picioroanu, C., Wimpenny, J.W.T., van Loosdrecht, M.C.M., 2001. Individual-based modelling of biofilms. *Microbiology* 147, 2897–2912.
- Laspidou, C.S., Kungolos, A., Samaras, P., 2010. Cellular-automata and individual-based approaches for the modeling of biofilm structures: pros and cons. *Desalination* 250 (1), 390–394.
- Lesne, A., 2006. Multiscale approaches. In: Françoise, G.N.J.P., Tsun, T.S. (Eds.), *Encyclopedia of Mathematical Physics*. Elsevier, Amsterdam, pp. 465–482.
- A. Lesne, 2013. Multiscale analysis of biological systems, *Acta Biotheoretica* 61, in press.
- Mabrouk, N., Deffuant, G., Tolker-Nielsen, T., Lobry, C., 2010. Bacteria can form interconnected microcolonies when a self-excreted product reduces their surface motility: evidence from individual-based model simulations. *Theory in Biosciences* 129 (1), 1–13.
- Mabrouk, N., 2010. Analyzing individual-based models of microbial systems. Ph.D. Thesis. Université Blaise Pascal de Clermont-Ferrand.
- Picioroanu, C., van Loosdrecht, M.C.M., Heijnen, J.J., 1998. A new combined differential-discrete cellular automaton approach for biofilm modeling: application for growth in gel beads. *Biotechnology and Bioengineering* 57 (6), 718–731.
- Torquato, S., 2002. *Random Heterogeneous Materials: Microstructure and Macroscopic Properties*. Springer, New-York.
- Wang, Q., Zhang, T., 2010. Review of mathematical models for biofilms. *Solid State Communications* 150 (21–22), 1009–1022.
- Wanner, O., Eberl, H.J., Morgenroth, E., Noguera, D., Picioroanu, C., Rittmann, B., van Loosdrecht, M.C.M., 2006. *Mathematical Modeling of Biofilms*. IWA Publishing Edition, London.
- Weinan, E., Engquist, B., 2003. The heterogeneous multiscale methods. *Communications in Mathematical Sciences* 1, 87–133.
- Weinan, E., Ren, W., Vanden-Eijnden, E., 2009. A general strategy for designing seamless multiscale methods. *Journal of Computational Physics* 228 (15), 5437–5453.